Supplementary Materials **Energy Materials**

Quasi-solid polymer electrolytes with binary and ternary salt mixtures for high-voltage lithium metal batteries

Nicola Boaretto[1,*], Oihane Garcia-Calvo[2], Mónica Cobos[2], Asier Fernandez de Añastro[1], Marta Diez Viera[1], Mustafa al Sammarraie Shakir[1], Simon Lindberg[1], Rosalía Cid[1], Gérôme Godillot[3], Leif Olav Jøsang[4], Andriy Kvasha[2], María Martínez-Ibañez[1]

[1]Centre for Cooperative Research on Alternative Energies CIC energiGUNE, Basque Research and Technology Alliance (BRTA), Vitoria-Gasteiz 01510, Spain.
[2]CIDETEC, Basque Research and Technology Alliance (BRTA), Donostia-San Sebastian 20014, Spain.
[3]Arkema, Groupement de Recherches de Lacq, Lacq 64170, France.
[4]Cerpotech, Kvenildmyra 6, Heimdal 7093, Norway.

Correspondence to: Dr. Nicola Boaretto, Centre for Cooperative Research on Alternative Energies CIC energiGUNE, Basque Research and Technology Alliance (BRTA), Alava Technology Park, Albert Einstein 48, Vitoria-Gasteiz 01510, Spain. *E-mail:* nboaretto@cicenergigune.com

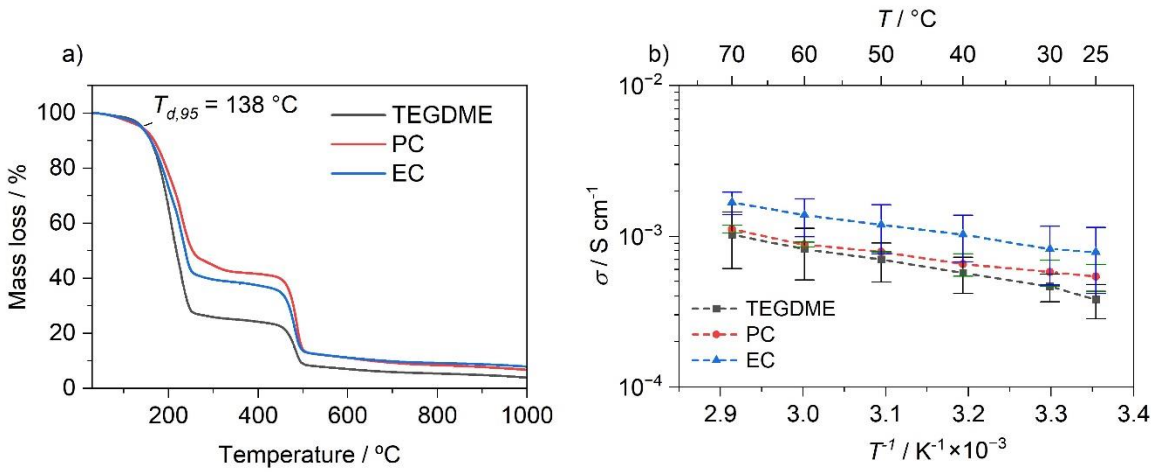

Figure S1. Thermogravimetric (a) and ionic conductivity (b) profiles of unsupported QSPEs with different plasticizers, with LiFSI as lithium salt, and prepared with acetone as processing solvent.

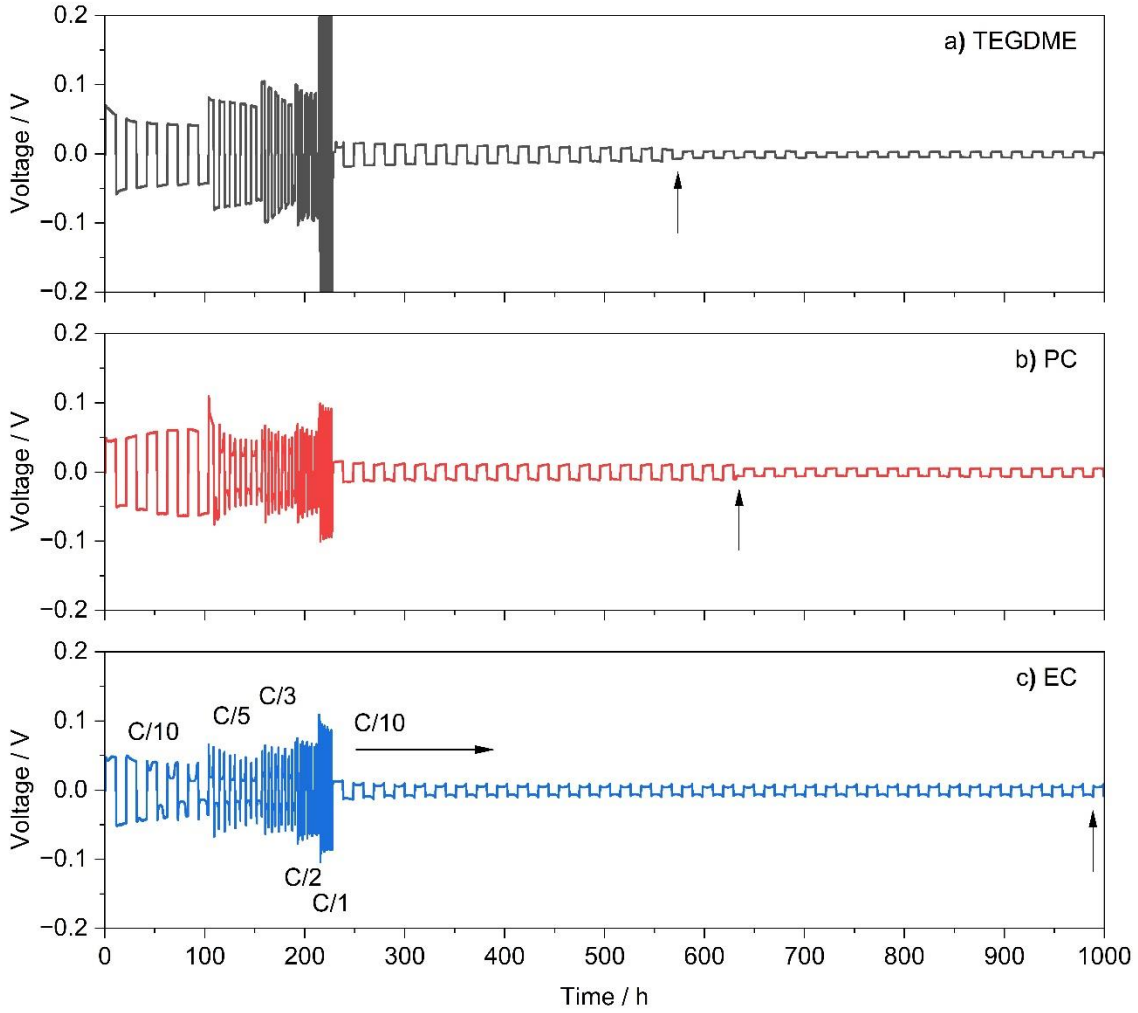

Figure S2. Plating/stripping profiles of Li||Li cells with unsupported QSPEs, and with 500 µm-thick Li electrodes. Unsupported QSPEs were prepared with LiFSI as lithium salt, and with acetone as processing solvent. Cycling was performed at room temperature and at a plated/stripped capacity of 1 mAh cm^{-2}. Electrolyte plasticizers: a) TEGDME; b) PC; c) EC.

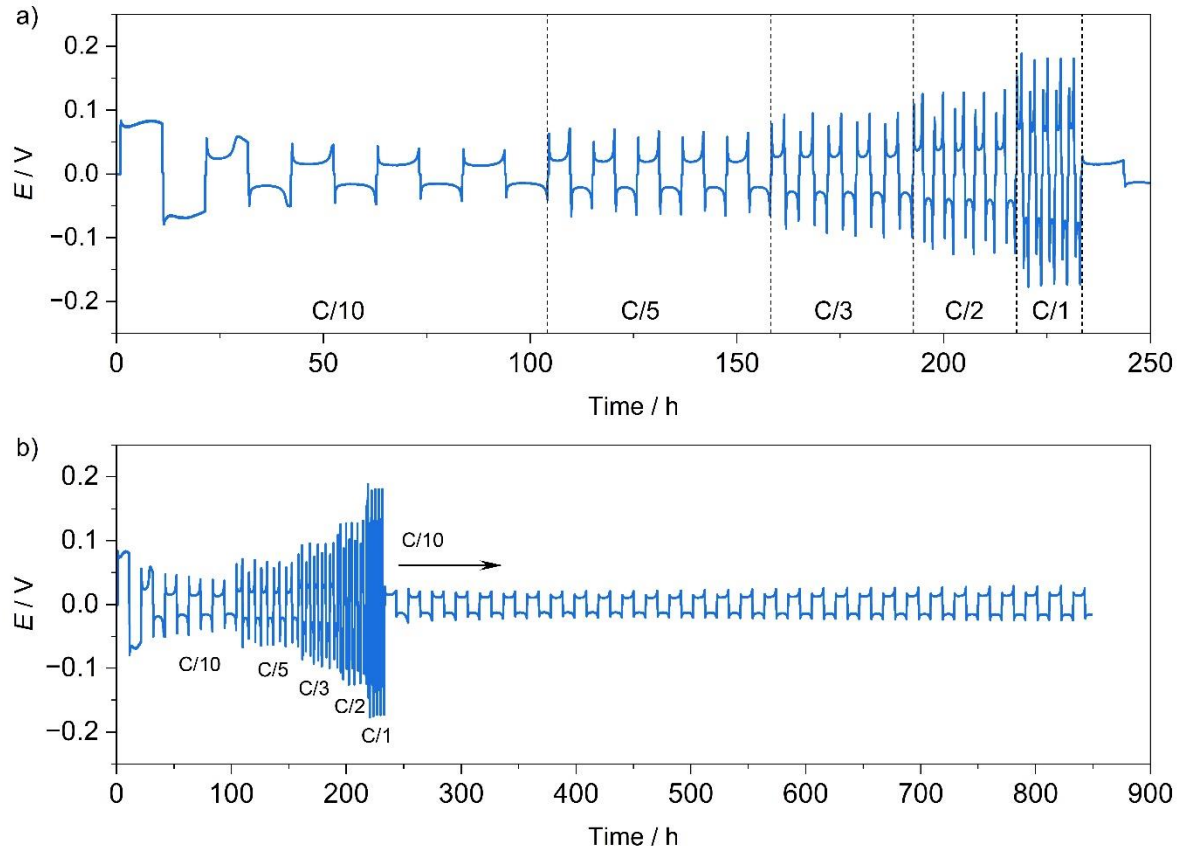

Figure S3. Plating/stripping profiles of Li||Li cells with unsupported QSPE, EC as electrolyte plasticizer, LiFSI as lithium salt, and with thin Li-Cu electrodes. Cycling was performed at room temperature and at a plated/stripped capacity of 1 mAh cm^{-2}.

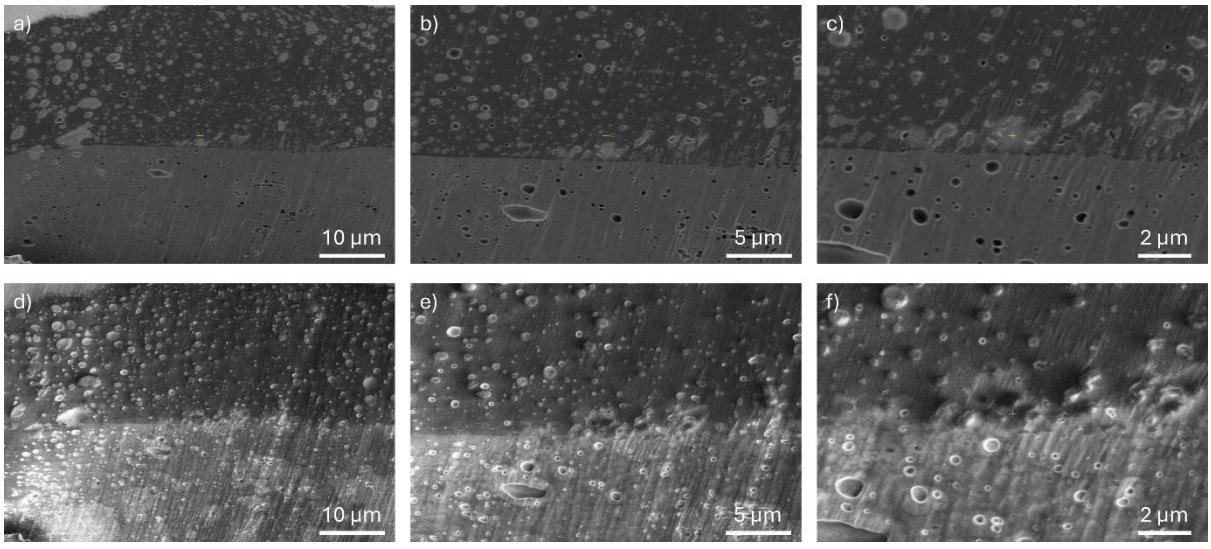

Figure S4. Cross-section SEM images of a supported QSPE, at the interface between the infiltrated polyolefin microporous separator (bottom) and the overlaying QSPE layer (top), obtained at an acceleration voltage of 2 kV. a – c) Images obtained with an in-lens detector at a) 7k×, b) 14k×, and c) 14k× magnification; d – f) Images obtained with an in-column detector at a) 7k×, b) 14k×, and c) 14k× magnification.

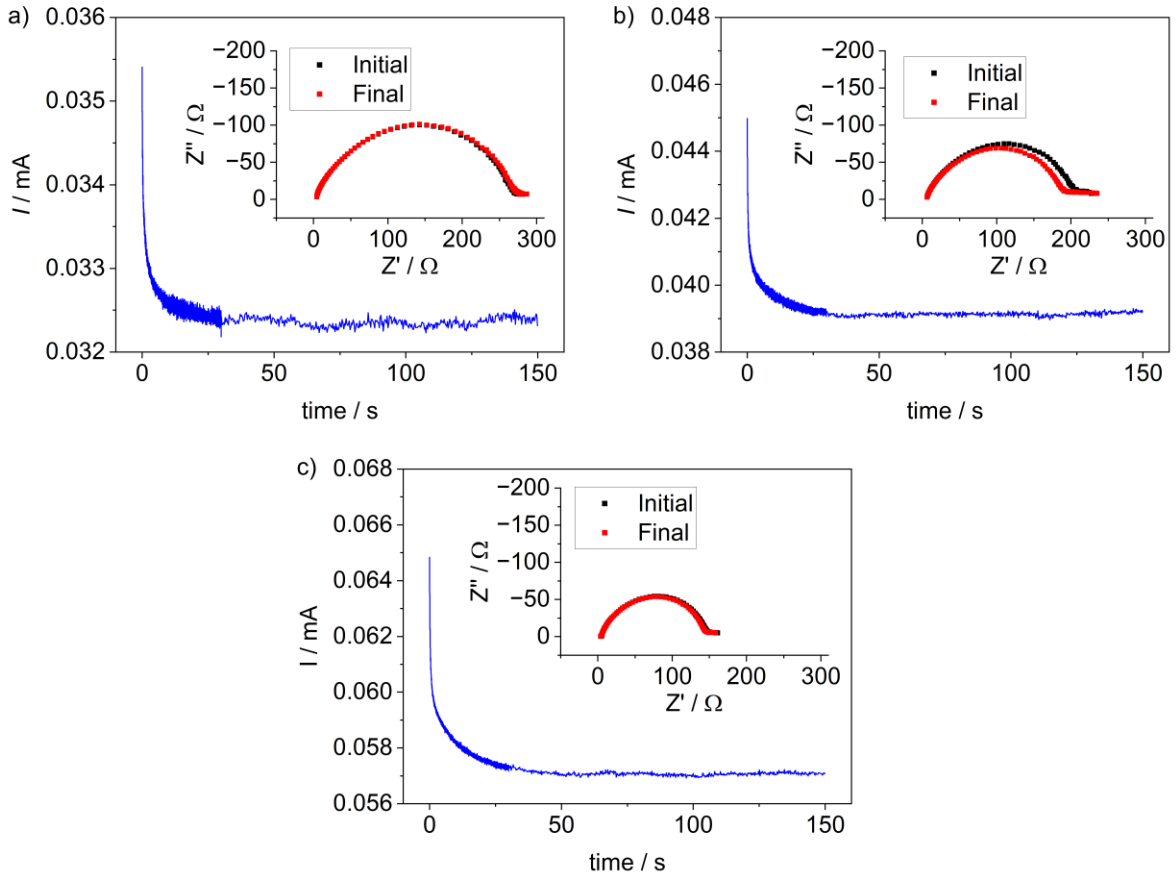

Figure S5. Chronoamperometric profiles of Li||Li cells at 25 °C and ΔV = 10 mV. During the first 30 s, the record frequency was one point every 10 ms. Afterwards, one point every 200 ms. The insets show the EIS spectra collected before and after the chronoamperometries. a) QSPE-1; b) QSPE-2; c) QSPE-3.

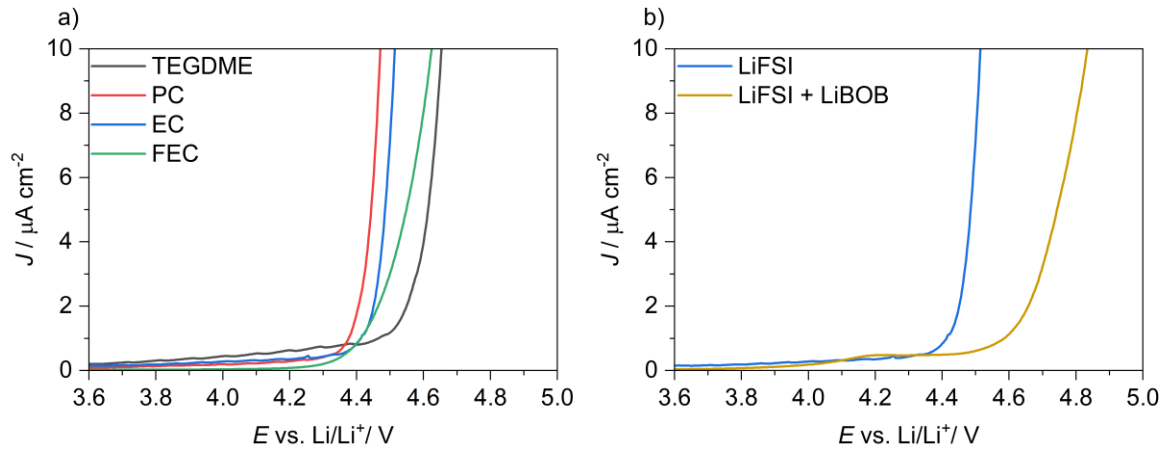

Figure S6. LSV profiles of SS||Li cells with unsupported QSPEs, collected at room temperature and at 0.1 mV s^{-1}. a) QSPEs with LiSFI as main salt, and different plasticizers; b) EC as plasticizer, LiFSI and mixture of LiFSI/LiBOB.

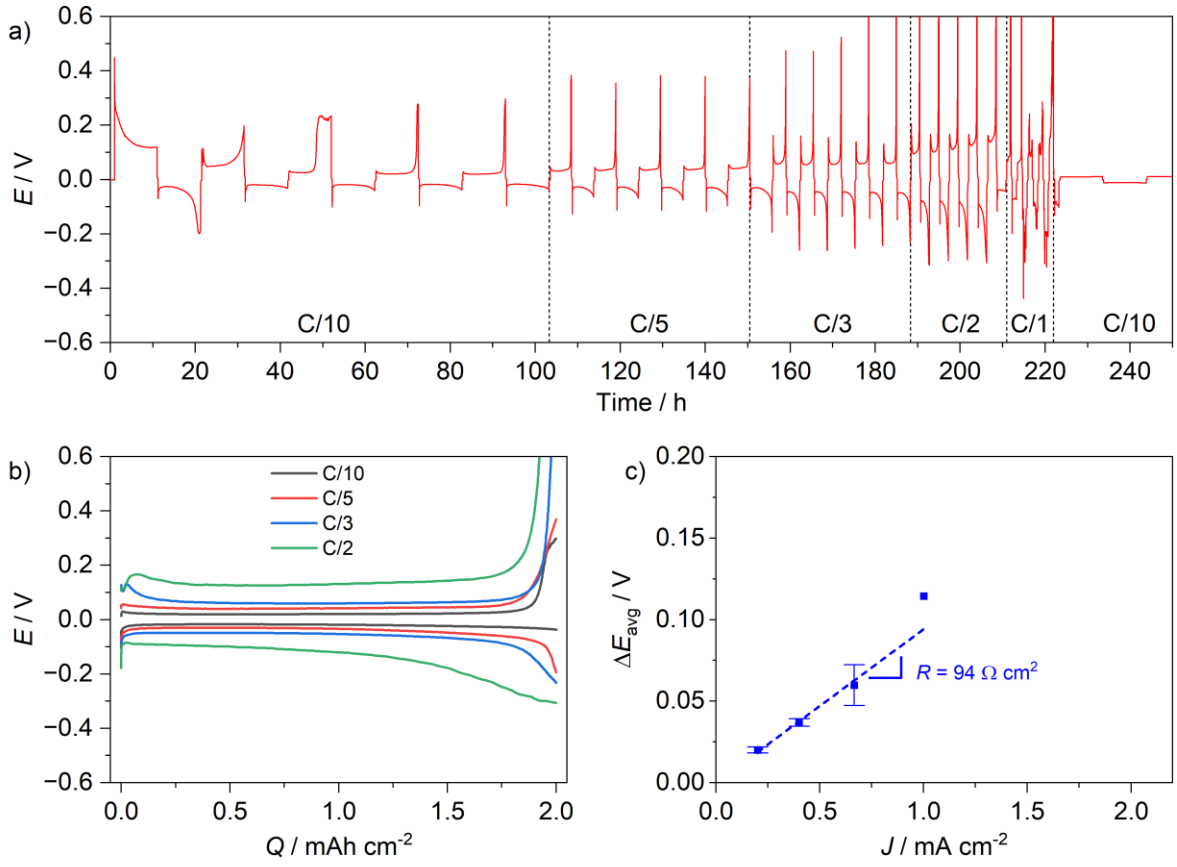

Figure S7. Plating/stripping performance of a Li-Cu|QSPE-1|Li-Cu cell at room temperature and with plated/stripped capacity of 2 mAh cm^{-2}. a) Voltage vs. time profile. Short circuit was observed in the last cycle at C/2; b) voltage *vs.* capacity profiles at different C-rates (fifth cycle at each C-rate, fourth cycle at C/2); c) average plateau voltage *vs.*current density. The slope was used to estimate the internal cell resistance in steady-state conditions.

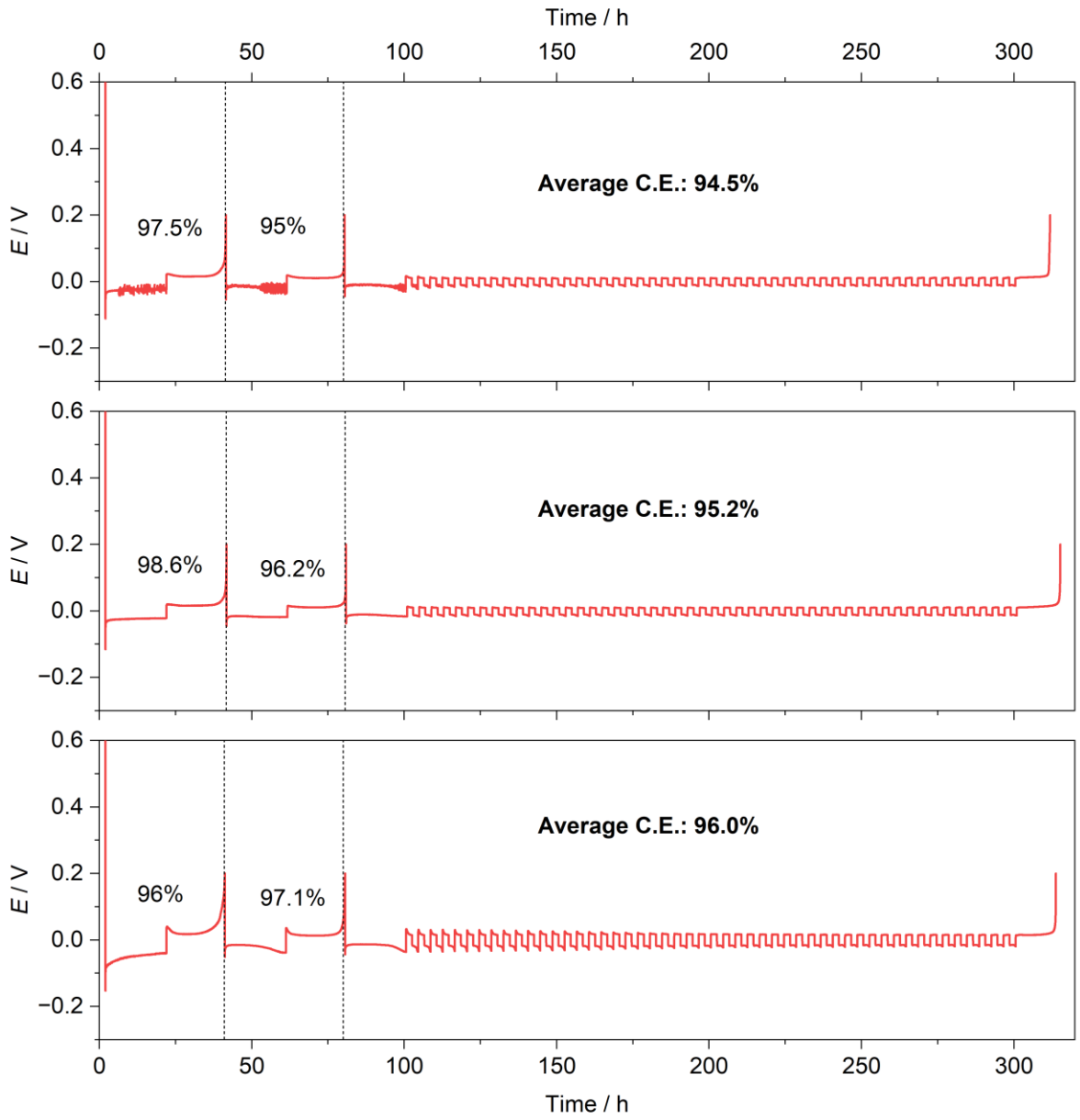

Figure S8. Voltage *vs.* time profiles of Cu|QSPE-2|Li cells (three replicas). The average coulombic efficiency during the intermediate short cycles is indicated in bold. The coulombic efficiency of the first two conditioning cycles is also indicated.

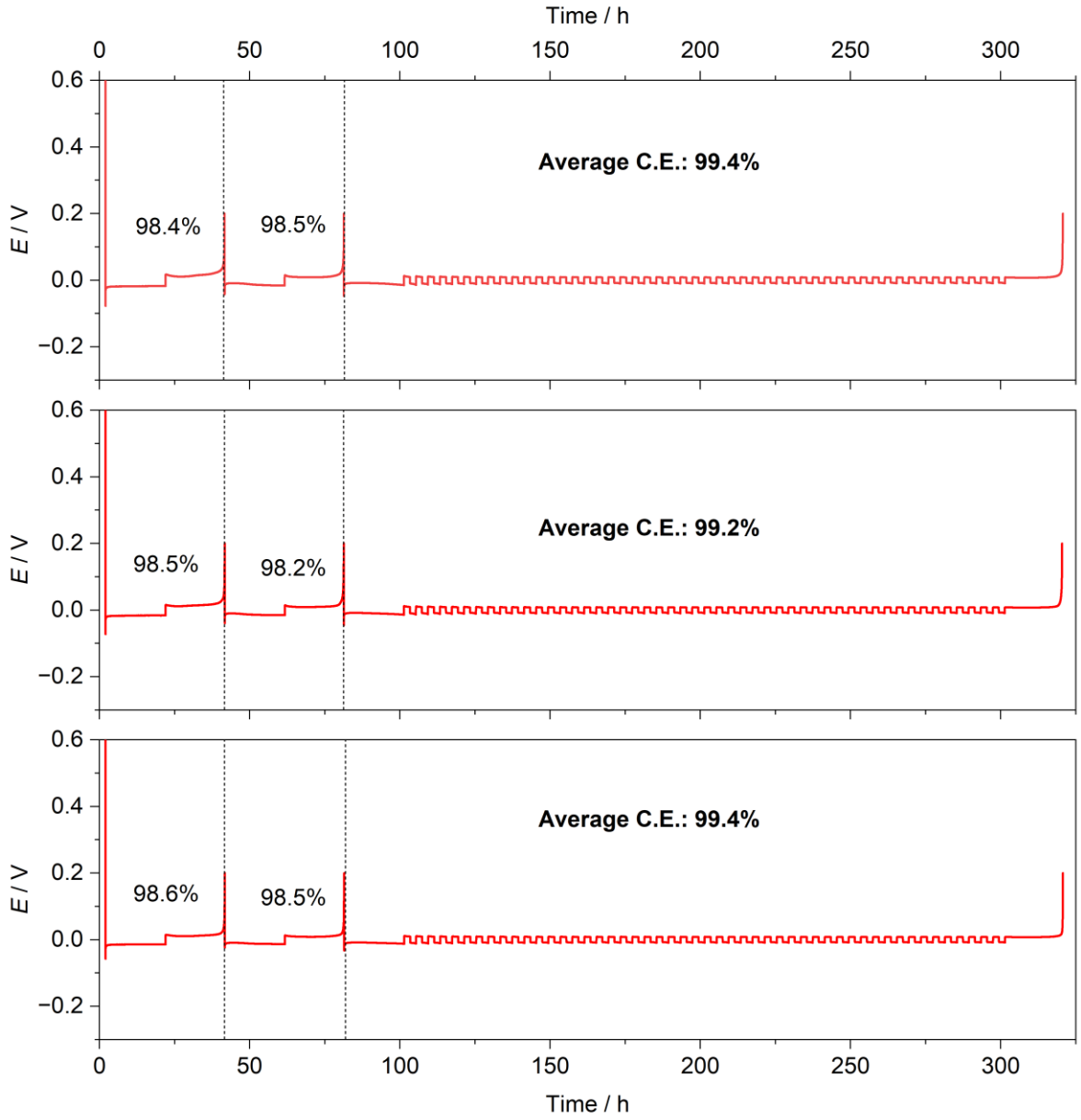

Figure S9. Voltage *vs.* time profiles of Cu|QSPE-3|Li cells (three replicas). The average coulombic efficiency during the intermediate short cycles is indicated in bold. The coulombic efficiency of the first two conditioning cycles is also indicated.

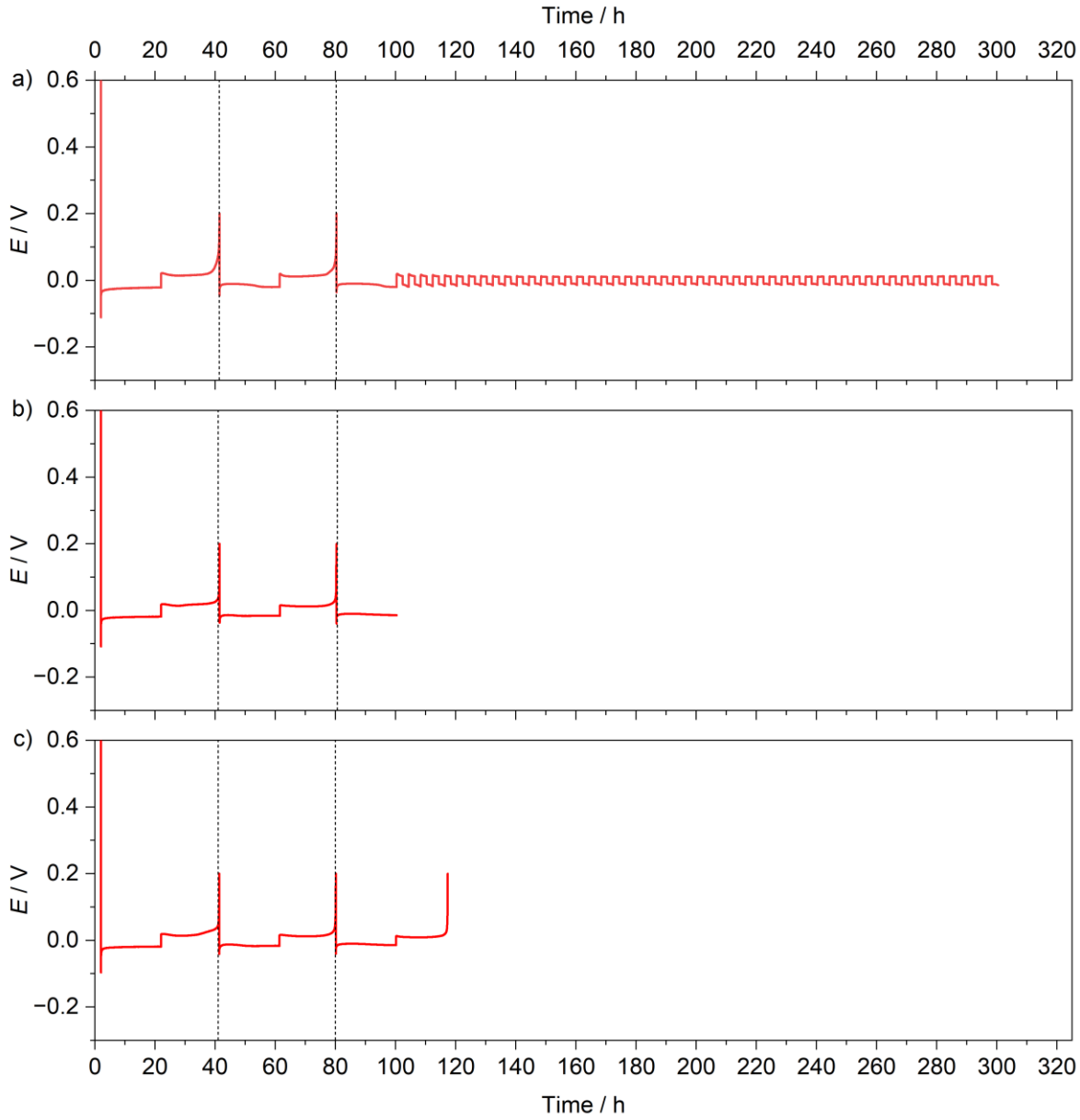

Figure S10. Voltage *vs.* time profiles of Cu|QSPE-2|Li cells cycled for XPS experiments. Galvanostatic cycling was performed at room temperature. The long cycles were carried out at 2 mAh cm^{-2}, and at 0.1 mA cm^{-2}. Short cycles were performed at 0.2 mAh cm^{-2}, and at 0.1 mA cm^{-2}. a) Long-cycled electrode; b) fully plated electrode; c) fully stripped electrode.

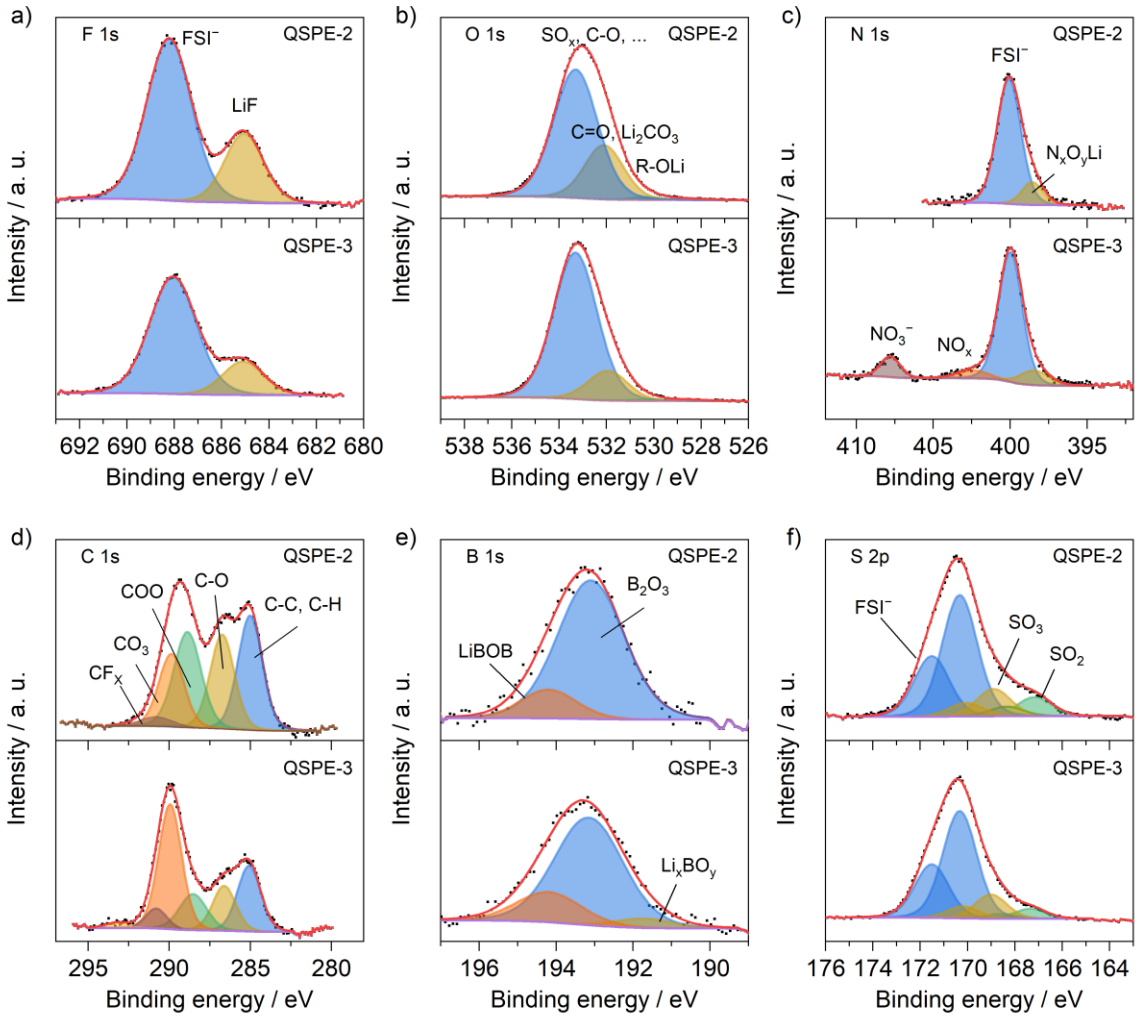

Figure S11. X-ray photoelectron spectra of fully stripped Cu electrodes recovered from Cu||Li cells, cycled either with QSPE-2 or QSPE-3 as electrolyte. Cycling was performed at room temperature, with three cycles (stripped state) at 2 mAh cm^{-2} and 0.1 mA cm^{-2}. The spectra obtained with QSPE-2 are shown in the upper panels, those with QSPE-3 in the lower panels. a) F 1s, b) O 1s, c) N 1s, d) C 1s, e) B 1s and f) S 2p photoelectron peaks.

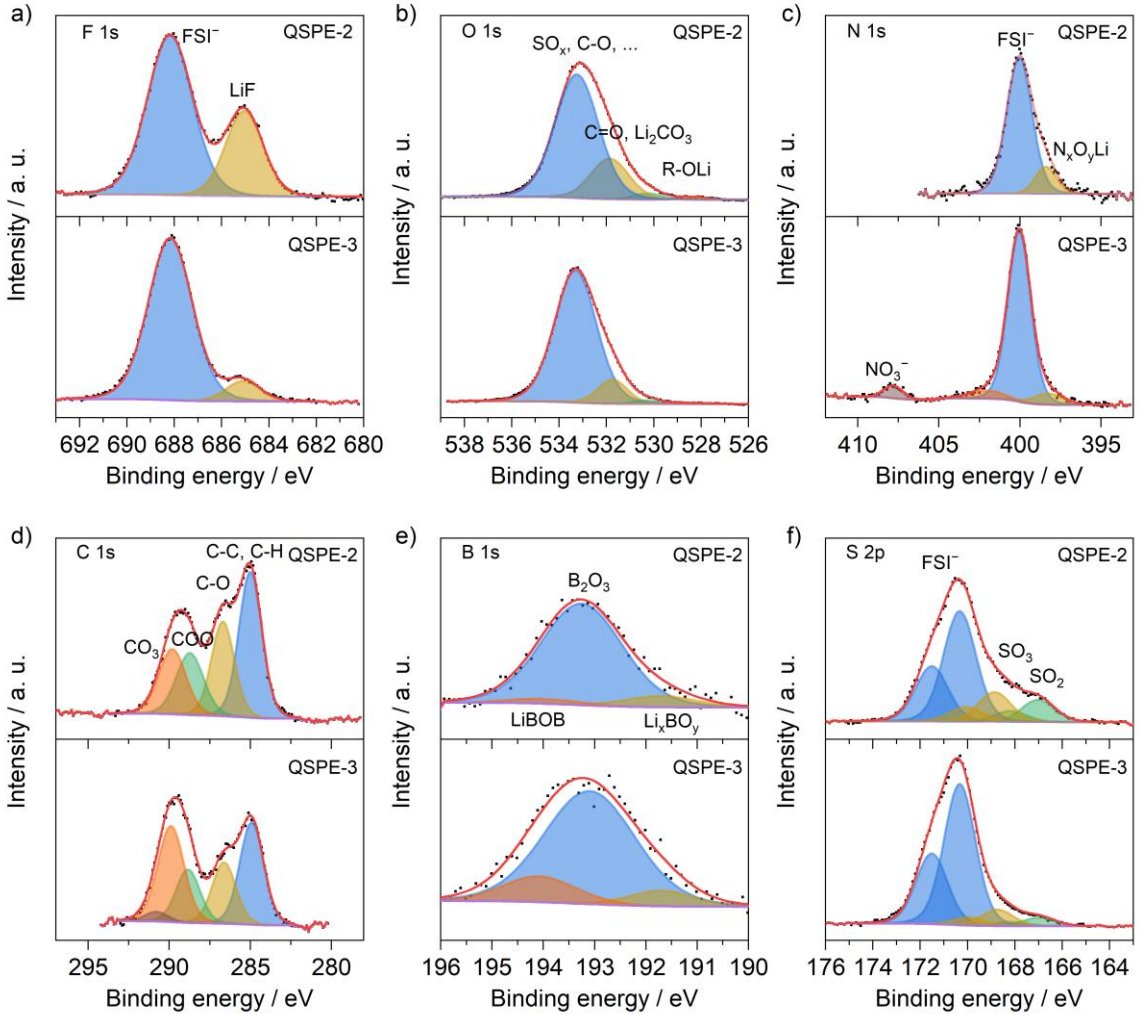

Figure S12. X-ray photoelectron spectra of fully plated Cu electrodes recovered from Cu||Li cells, cycled either with QSPE-2 or QSPE-3 as electrolyte. Cycling was performed at room temperature, with two and a half cycles (plated state) at 2 mAh cm^{-2} and 0.1 mA cm^{-2}. The spectra obtained with QSPE-2 are shown in the upper panels, those with QSPE-3 in the lower panels a) F 1s, b) O 1s, c) N 1s, d) C 1s, e) B 1s and f) S 2p photoelectron peaks.

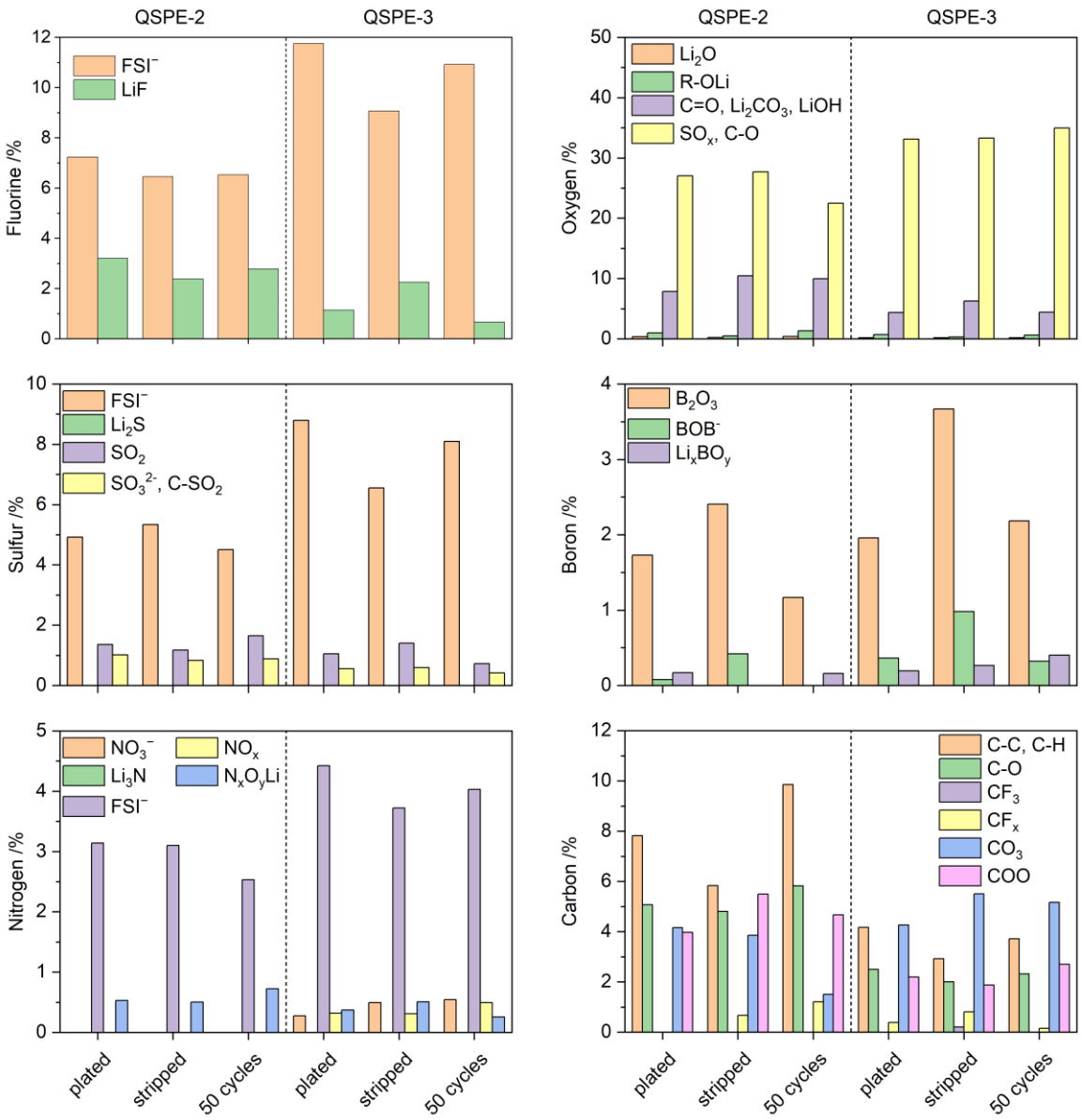

Figure S13. Relative concentration of the different species obtained from deconvolution of the XPS spectra of Cu electrodes, after two and a half cycles at 2 mAh cm^{-2} and 0.1 mA cm^{-2} (plated), three cycles in the same conditions (stripped), and after 50 cycles at 0.2 mAh cm^{-2} and 0.1 mA cm^{-2} (50 cycles).

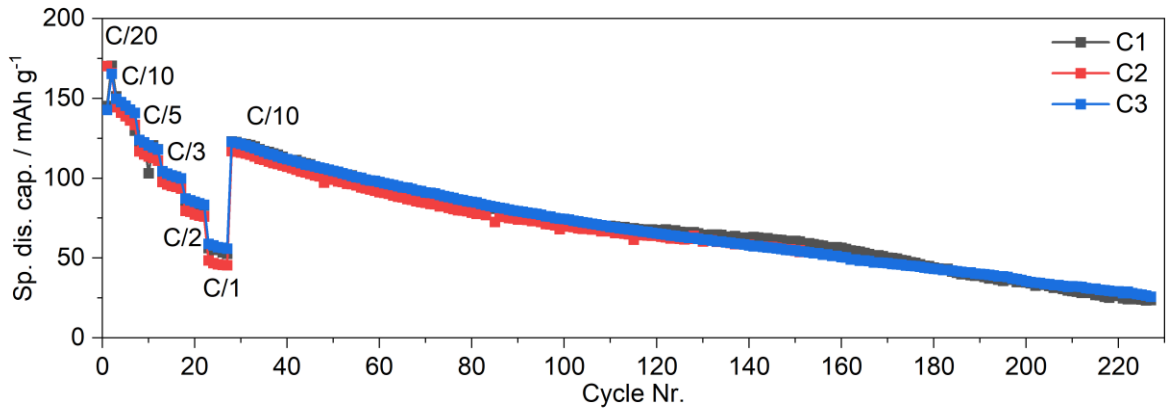

Figure S14. Specific discharge capacity of three NMC-811||Li-Cu coin cells with QSPE-3 as electrolyte, cycled at room temperature, with cathode active material loading of ~13 mg cm^{-2}.

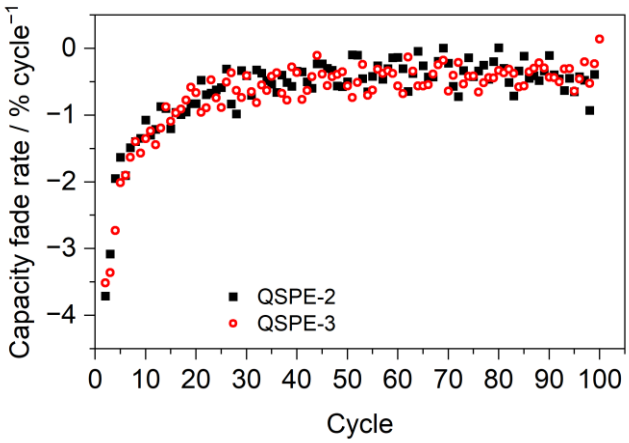

Figure S15. Rate of capacity fade of two NMC-811||Li-Cu coin cells, with QSPE-2 and QSPE-3 as electrolytes, cycled at room temperature, between 3.0 V and 4.3 V, and at constant C-rate of C/10. The active material loading was of ~13 mg cm^{-2}.

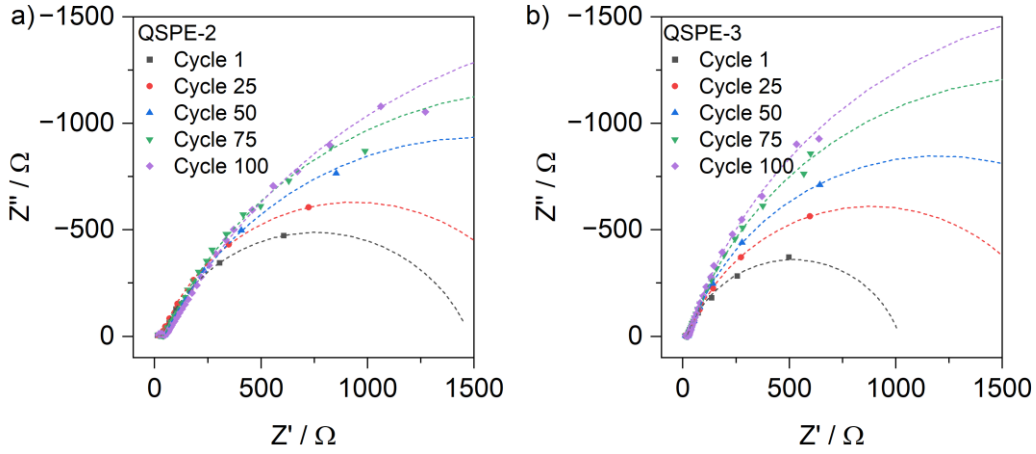

Figure S16. Selected EIS spectra of NMC-811||Li-Cu cells with a) QSPE-2 and b) QSPE-3, upon cycling at room temperature, between 3.0 V and 4.3 V, and at constant C-rate of C/10. Dashed lines represent the fitting curves, in an extended frequency range (1 MHz to 0.001 Hz).

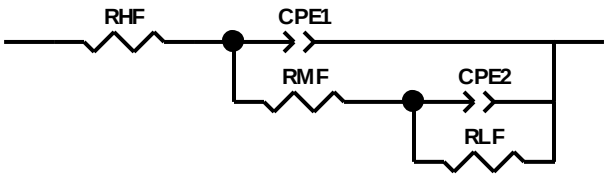

Figure S17. Equivalent circuit model used to fit the EIS spectra of NMC-811||Li-Cu cells in Figure S16.

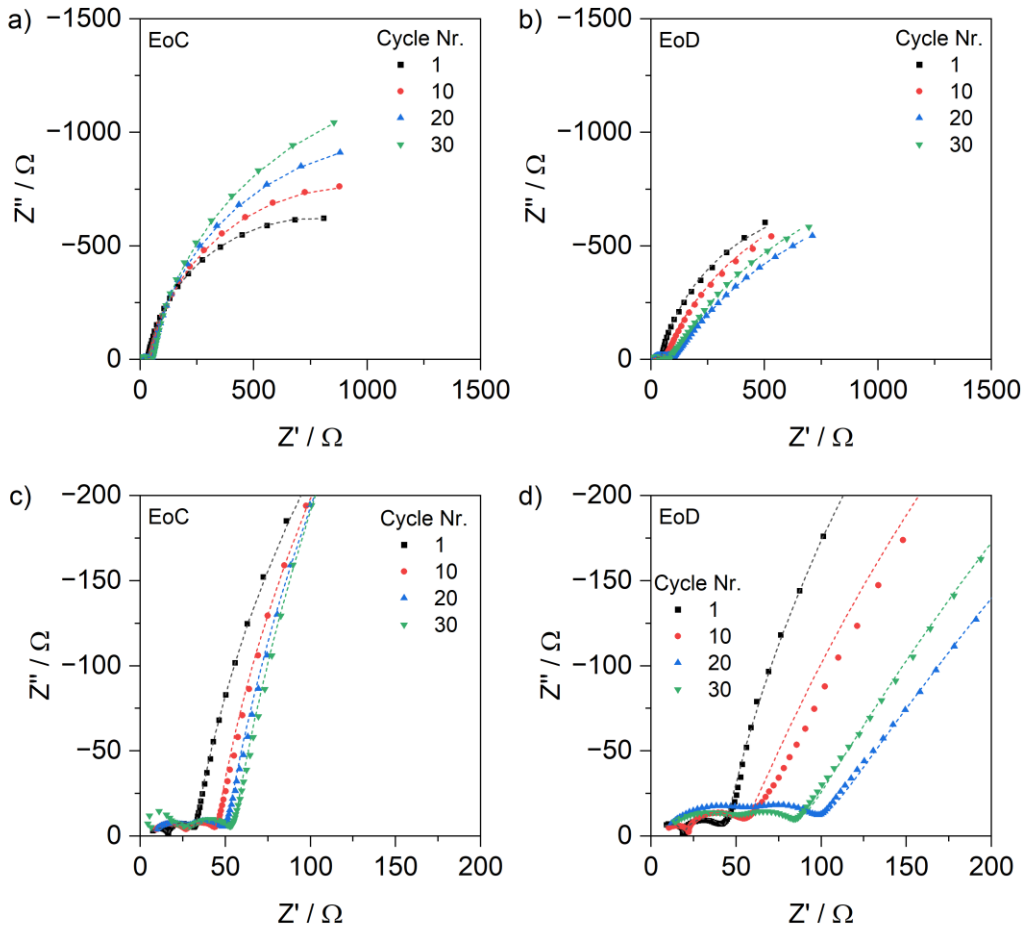

Figure S18. Selected EIS spectra (positive electrode spectra) of a three electrode NMC-811||Li-Cu cell, with QSPE-2 as electrolyte, upon cycling at C/20 (cycle 1: first cycle at C/20). a) Spectra at the end of charge (EoC); b) spectra at the end of discharge (EoD); c) zoom on the high/middle-frequency region at the EoC; d) zoom on the high/middle-frequency region at the EoD. The EIS spectra were collected after one hour resting. Dashed lines represent the fitting curves.

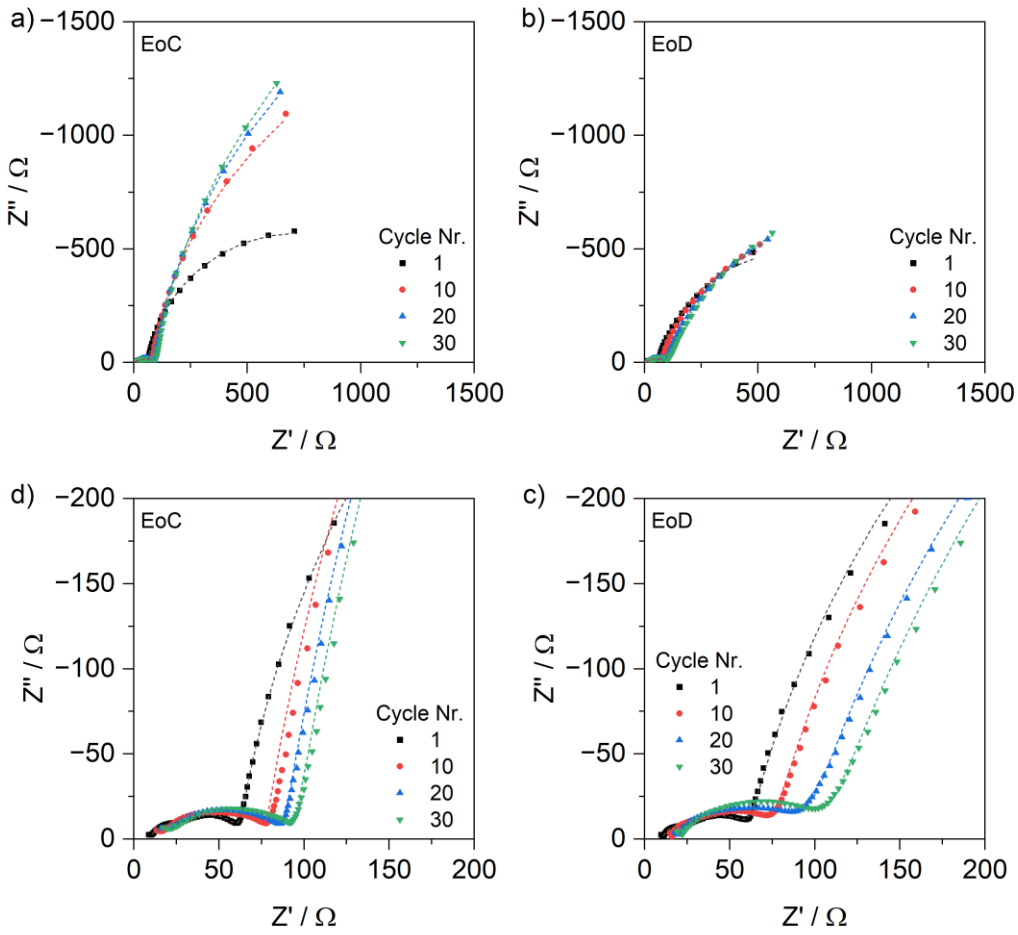

Figure S19. Selected EIS spectra (positive electrode spectra) of a three electrode NMC-811||Li-Cu cell, with QSPE-3 as electrolyte, upon cycling at C/20 (cycle 1: first cycle at C/20). a) Spectra at the end of charge (EoC); b) spectra at the end of discharge (EoD); c) zoom on the high/middle-frequency region at the EoC; d) zoom on the high/middle-frequency region at the EoD. The EIS spectra were collected after one hour resting. Dashed lines represent the fitting curves.

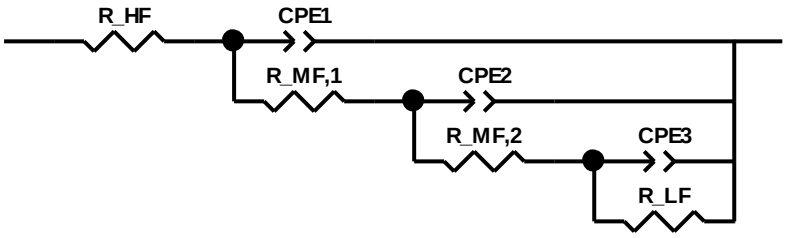

Figure S20. The equivalent circuit model used to fit the EIS spectra of NMC-811||Li-Cu three-electrode cells.

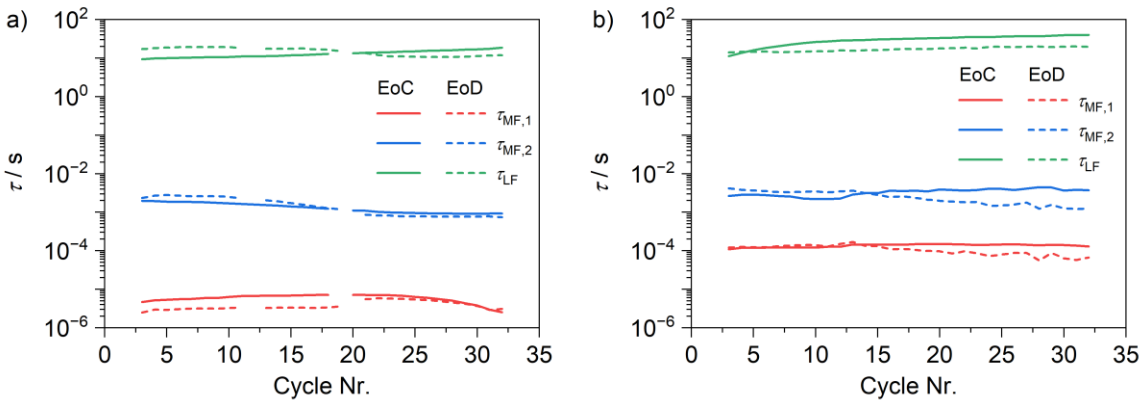

Figure S21. Characteristic time constants of the polarization phenomena associated with the positive electrodes EIS spectra of NMC-811||Li-Cu cells with a) QSPE-2, and b) QSPE-3.